On the range of the first two Dirichlet and Neumann eigenvalues of the Laplacian

Pedro R.S. Antunes, Antoine Henrot

ON THE RANGE OF THE FIRST TWO DIRICHLET AND NEUMANN EIGENVALUES OF THE LAPLACIAN

PEDRO R. S. ANTUNES AND ANTOINE HENROT

Abstract. In this paper we study the set of points, in the plane, defined by $\{(x,y) = (\lambda_1(\Omega), \lambda_2(\Omega)),\ |\Omega| = 1\}$, where $(\lambda_1(\Omega), \lambda_2(\Omega))$ are either the two first eigenvalues of the Dirichlet-Laplacian, or the two first non trivial eigenvalues of the Neumann-Laplacian. We consider the case of general open sets together with the case of convex open domains. We give some qualitative properties of these sets, show some pictures obtained through numerical computations and state several open problems.

1. Introduction

Let $\Omega \subset \mathbb{R}^2$ be a bounded open set and consider the Dirichlet eigenvalue problem,

$$\begin{cases} -\Delta u = \lambda u & \text{in } \Omega \\ u = 0 & \text{on } \partial\Omega, \end{cases} \tag{1}$$

defined on the Sobolev space $H_0^1(\Omega)$. We will denote the eigenvalues by $0 < \lambda_1(\Omega) \leq \lambda_2(\Omega) \leq ...$ (counted with their multiplicities) and the corresponding orthonormal real eigenfunctions by $u_i,\ i = 1, 2, ...$ In [WK] and [BBF], it was studied the region

$$\mathcal{E}^D = \left\{(x,y) \in \mathbb{R}^2 : (x,y) = (\lambda_1(\Omega), \lambda_2(\Omega)),\ \Omega \subset \mathbb{R}^2, |\Omega| = 1\right\},$$

which is the range of the first two Dirichlet eigenvalues of planar sets with unit area. We also refer to [LY] for a similar study for the three first eigenvalues. Let us begin with some elementary facts. Obviously $\mathcal{E}^D$ lies in the first quadrant and within the sector $0 < x \leq y$, because we defined the eigenvalues to be ordered. The behavior of eigenvalues with respect to homothety ($\lambda_k(t\Omega) = \lambda_k(\Omega)/t^2$) has two consequences. First we can also write $\mathcal{E}^D = \left\{(x,y) \in \mathbb{R}^2 : (x,y) = (|\Omega|\lambda_1(\Omega), |\Omega|\lambda_2(\Omega)),\ \Omega \subset \mathbb{R}^2\right\}$. Then, it is clear that the region $\mathcal{E}^D$ is conical with respect to the origin in the sense,

$$(x,y) \in \mathcal{E}^D \Rightarrow (\alpha x, \alpha y) \in \mathcal{E}^D,\ \forall \alpha \geq 1,$$

(consider a homothety of ratio $1/\sqrt{\alpha}$ of the original domain and complete with a collection of small balls to reach volume 1 without changing the two first eigenvalues). Now, we can get more precise information about $\mathcal{E}^D$ thanks to some important results on the low eigenvalues of the Laplacian. This region can be reduced using

Date: August 21, 2010.

1991 *Mathematics Subject Classification.* Primary 35P15; Secondary 58G25.

Key words and phrases. Dirichlet Laplacian, Neumann Laplacian, eigenvalues, shape optimization.

The work of P.A. is partially supported by FCT, Portugal, through the scholarship SFRH/BPD/47595/2008, the scientific projects PTDC/MAT/101007/2008, FCT/CNRS and by Fundação Calouste Gulbenkian through program *Estímulo à Investigação 2009.* The work of A.H. is partially supported by ANR GAOS.

the famous Faber-Krahn inequality proved in [F1] and [K] which states that the ball minimizes λ_1 among all planar domains with the same area. We can write this result as

$$|\Omega|\lambda_1(\Omega) \geq \lambda_1(\mathcal{B}) = \pi j_{0,1}^2 \approx 18.16842,$$

where $j_{n,k}$ denotes the k-th positive zero of the Bessel function J_n and $\mathcal{B}$ denotes the ball of unit area. Equality holds if and only if Ω is a ball (up to a set of zero capacity). For the second eigenvalue, we know that the minimum is attained by two balls of equal area. This result is due to Krahn and has been rediscovered by Szegö, cited in [P1] and some other authors, see [H] for more details. It can be written as

$$|\Omega|\lambda_2(\Omega) \geq 2\lambda_1(\mathcal{B}) = 2\pi j_{0,1}^2 \approx 36.33684.$$

The quotient λ_2/λ_1 is maximized at the ball (cf. [AB1]), or equivalently,

$$\frac{\lambda_2(\Omega)}{\lambda_1(\Omega)} \leq \frac{\lambda_2(\mathcal{B})}{\lambda_1(\mathcal{B})} = \frac{j_{1,1}^2}{j_{0,1}^2} \approx 2.539.$$

It is also known that the set $\mathcal{E}^D$ is convex in the x-direction,

$$(x, y) \in \mathcal{E}^D \Rightarrow ((1-t)x + ty, y) \in \mathcal{E}^D, \ \forall t \in [0,1]$$

and in the y-direction

$$(x, y) \in \mathcal{E}^D \Rightarrow (x, (1-t)y + tx) \in \mathcal{E}^D, \ \forall t \in [0,1]$$

and is closed (cf. [BBF]). Moreover, the tangents at the extremal points are vertical (at the ball) and horizontal (at two balls) (cf [WK]). The above results show that the only unknown part of the set $\mathcal{E}^D$ is the lower part, the curve joining the points corresponding to one ball and two balls. In Figure 1, we have determined numerically this curve with the same procedure as in [WK], solving a minimization problem with a convex combination of λ_1 and λ_2. Our results were obtained with the gradient method to solve the minimization problems, as in [AA2]. The solver that we used was the Method of Fundamental Solutions (MFS), as studied in [AA1] or in some cases an enriched version of the MFS, as in [AV]. We recall the conjecture

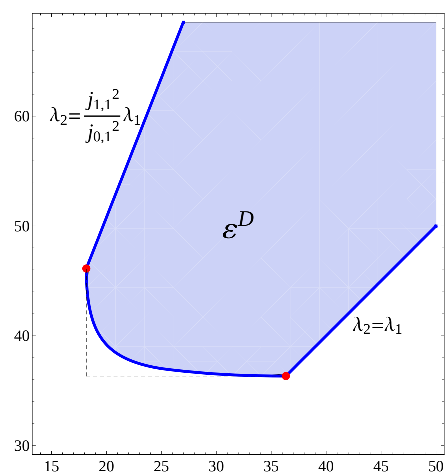

FIGURE 1. The region $\mathcal{E}^D$.

already stated in [BBF]:

Conjecture 1. The set $\mathcal{E}^D$ is convex.

The plan of this paper is the following. In the next section we study the subset $\mathcal{E}^D_C$ of $\mathcal{E}^D$ corresponding to convex domains. We look at the case of some particular polygons, we prove that $\mathcal{E}^D_C$ is closed, connected by arcs and give some information on its boundary. In section 3 the case of Neumann eigenvalues for general domains is considered. We describe a part of its boundary and some other qualitative properties. Finally, in section 3.2 we address a similar study for the first two nontrivial Neumann eigenvalues of convex domains. We prove, in particular, that the convex domain which maximizes the second (non trivial) Neumann eigenvalue is not a stadium.

2. The Dirichlet case with convex domains

In this section we are interested in the subset of $\mathcal{E}^D$ obtained for convex sets,

$$\mathcal{E}^D_{\mathcal{C}} = \left\{(x,y) \in \mathbb{R}^2 : (x,y) = (\lambda_1(\Omega), \lambda_2(\Omega)),\ \Omega \subset \mathbb{R}^2, |\Omega| = 1,\ \Omega \text{ convex}\right\}.$$

We start by some numerical results obtained for particular classes of convex polygons.

2.1. **The case of convex polygons.** In this section we present some numerical results for polygonal convex domains. We generated randomly a sample of convex polygons and calculated the first two Dirichlet eigenvalues. Our sample has 4500 triangles, 23000 quadrilaterals and 45000 octagons. We will see that it is convenient to distinguish two types of isosceles triangles, which play a different role in the region $\mathcal{E}^D_{\mathcal{C}}$. For this purpose we recall a definition introduced in [AF2], but instead of the terminology used in that paper we will follow [LS1].

Definition 2.1. The aperture of an isosceles triangle is the angle between its two equal sides. Call a triangle subequilateral if it isosceles with aperture less than $\pi/3$, and superequilateral if it is isosceles with aperture greater that $\pi/3$.

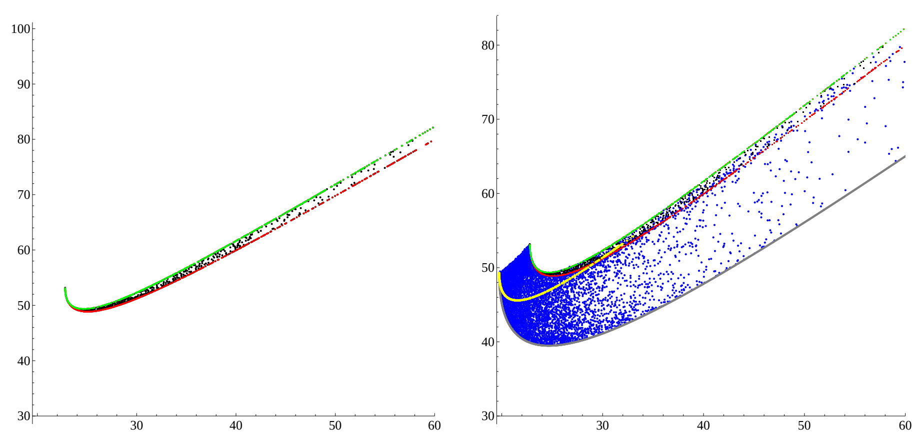

FIGURE 2. The range of the first two Dirichlet eigenvalues for triangles (left) and convex quadrilaterals (right).

In Figure 2-left we plot the subregion of $\mathcal{E}_{\mathcal{C}}^{D}$ that we obtain for triangles. The numerical results indicate that the region is delimited above (resp. bellow) by the curve corresponding to superequilateral (resp. subequilateral) triangles which are marked in green (resp. in red). The minimum of λ_2 over all the superequilateral triangles is attained for the right triangle and the minimum of λ_2 among the subequilateral triangles, which is also the minimum over all triangles is attained for a triangle whose aperture is approximately equal to 0.5996796. It is well known (Pólya theorem, see [H]) that the minimum of λ_1 is attained for the equilateral triangle. This result is also illustrated in the Figure, where it can be seen that the minimum of λ_1 is attained at the intersection of the curves corresponding to subequilateral and superequilateral triangles, which is the equilateral triangle. It can be proved that the tangent to the region at the point of the equilateral triangle is vertical. In Figure 2-right we plot similar results obtained for convex quadrilaterals. We marked in yellow the rhomboidal domains and in gray the rectangles. It is straightforward to verify that the curve of the rectangles is defined by

$$\lambda_2=\frac{5\lambda_1-3\sqrt{\lambda_1^2-4\pi^4}}{2},\ \lambda_1\geq 2\pi^2 \tag{2}$$

and the numerical results that we gathered suggest that this is also the lower part of the boundary of the region that we obtain for convex quadrilaterals,

Conjecture 2. For a convex quadrilateral Q with unit area we have

$$\lambda_2(Q)\geq\frac{5\lambda_1(Q)-3\sqrt{\lambda_1^2(Q)-4\pi^4}}{2}.$$

Equality holds if Q is a rectangle.

The upper part of the boundary for $\lambda_1\geq 4\pi^2\sqrt{3}/3$ seems to correspond to the superequilateral triangles. For $2\pi^2\leq\lambda_1\leq 4\pi^2\sqrt{3}/3$ the upper boundary is defined by a curve of quadrilaterals with one symmetry (having $\lambda_2=\lambda_3$) which connects the square to the equilateral triangle. The fact that the rectangles and some type of isosceles triangles appear as extremal sets was already detected in [AF1], when studying isoperimetric bounds for $\lambda_1(\Omega)$ and in [AF2] for the spectral gap, $\lambda_2(\Omega)-\lambda_1(\Omega)$.

In Figure 3 we plot the results obtained for convex octagons. The regular polygons are marked with larger red points and the ball with a larger black point. Also in this case, the superequilateral triangles seem to be on the upper part of the boundary. We give below, in section 2.2 some conditions relating to the property for a domain to be on the boundary of $\mathcal{E}_{\mathcal{C}}^{D}$.

Conjecture 3. The superequilateral triangles are on $\partial\mathcal{E}_{\mathcal{C}}^{D}$.

A similar conjecture was proposed in [AF2] for the spectral gap. Now we present numerical results for the lower boundary of $\mathcal{E}_{\mathcal{C}}^{D}$. The results plotted in Figure 3 seem to suggest that we have a continuous family of rectangles on the lower part of the boundary, but in the next section we prove that this is not true. We determined numerically that part of the boundary and show the results in Figure 4. In blue we have the boundary of the region $\mathcal{E}_{\mathcal{C}}^{D}$ and with a dashed red line we marked the boundary of the region $\mathcal{E}^{D}$, already identified in Figure 1. We observed that for the general case of the region $\mathcal{E}^{D}$, in a neighborhood of the ball the domains that are in the lower part of $\partial\mathcal{E}^{D}$ are convex. Then, in that region the boundaries $\partial\mathcal{E}^{D}$

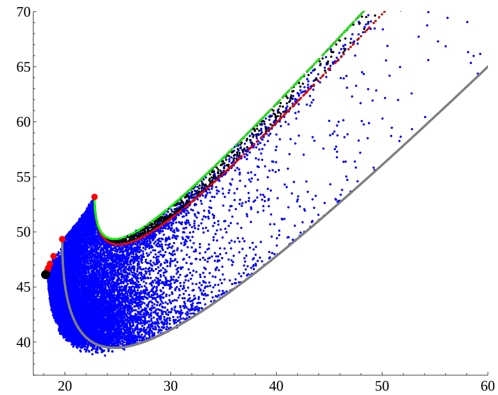

FIGURE 3. The range of the first two Dirichlet eigenvalues for octagons.

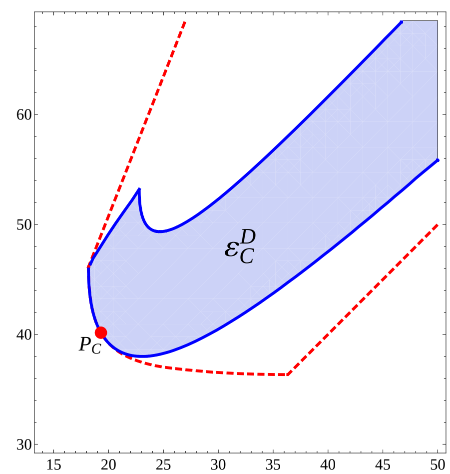

FIGURE 4. The region $\partial\mathcal{E}_{\mathcal{C}}^D$.

and $\partial\mathcal{E}_{\mathcal{C}}^D$ coincide. In Figure 4 we marked with a red point $P_{\mathcal{C}}$, the location where the two boundaries split into two distinct curves. In Figure 5 we plot a domain Ω with unit area for which we have $(\lambda_1(\Omega), \lambda_2(\Omega)) = P_{\mathcal{C}}$.

The lower point of the domain $\partial\mathcal{E}_{\mathcal{C}}^D$ already sparked off some study. In 1973, Troesch formulated in [T] the conjecture that the convex planar domain which minimize the second eigenvalue could be the stadium (the convex hull of two identical tangent balls). This conjecture was refuted by Henrot and Oudet in [HO2]. However, the analytic and numerical results presented in [HO1] and [O1] show that the optimal domain is very close to the stadium, not only from the numerical point of view, but also from a geometrical point of view. With our algorithm we obtained a numerical optimal convex domain with unit area for which one has $\lambda_2 \approx 37.987$ which is smaller that the corresponding value of the stadium for which we have $\lambda_2 \approx 38.002$. Our numerical optimal domain is plotted in Figure 15, together with the optimal convex domain for μ_2. In the next section we provide some analytical

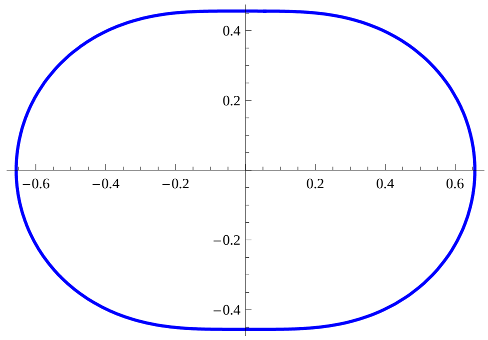

FIGURE 5. A domain Ω for which $(\lambda_1(\Omega), \lambda_2(\Omega)) = P_{\mathcal{C}}$.

results, namely a study of the properties of the domains that are on the boundary of the region $\mathcal{E}_{\mathcal{C}}^D$ and the tangents at some extremal points.

2.2. **Some qualitative results.** In this section we prove some results which describe to some extent the region $\mathcal{E}_{\mathcal{C}}^D$. The first property is of topological nature. Using continuity of eigenvalues of convex domains with respect to Hausdorff convergence, it is easy to prove that $\mathcal{E}_{\mathcal{C}}^D$ is closed and connected by arcs. Actually, it seems to be simply connected but it is probably much harder to prove. Now, the main point is to describe the boundary of the set $\mathcal{E}_{\mathcal{C}}^D$. We will say that a domain Ω is on the boundary of $\mathcal{E}_{\mathcal{C}}^D$ if the point $(|\Omega|\lambda_1(\Omega), |\Omega|\lambda_2(\Omega))$ lies on the boundary of $\mathcal{E}_{\mathcal{C}}^D$. We give in the theorem below, some necessary conditions for a domain Ω to be on the boundary of $\mathcal{E}_{\mathcal{C}}^D$. For sake of simplicity, we only consider the case of C^2 strictly convex domains and the case of polygons which are certainly the most significative ones. For intermediate cases, the idea is the same, but the statements would be more complicated.

Theorem 2.2. (1) *The region $\mathcal{E}_{\mathcal{C}}^D$ is unbounded, connected by arcs and closed.*

(2) *Let Ω be a C^2 domain, strictly convex, which is on the boundary of $\mathcal{E}_{\mathcal{C}}^D$ and assume that $\lambda_2(\Omega)$ is simple. Then the functions $1, |\nabla u_1|^2, |\nabla u_2|^2$ are linearly dependent on the boundary of Ω.*

(3) *Let Ω be a polygon with N sides which is on the boundary of $\mathcal{E}_{\mathcal{C}}^D$. Let us denote by $\gamma_k, k = 1 \dots N$ its sides and a_k the length of γ_k. Let us introduce the $2N$ plane vectors defined by*

$$V_k = \begin{pmatrix} a_k\lambda_1 - \int_{\gamma_k} |\nabla u_1|^2\,ds \\ a_k\lambda_2 - \int_{\gamma_k} |\nabla u_2|^2\,ds \end{pmatrix} \quad \text{and} \quad V_k' = \begin{pmatrix} a_k\lambda_1 - \int_{\gamma_k} s|\nabla u_1|^2\,ds \\ a_k\lambda_2 - \int_{\gamma_k} s|\nabla u_2|^2\,ds \end{pmatrix}. \tag{3}$$

Let us assume that $\lambda_2(\Omega)$ is simple. Then the $2N$ vectors V_k, V_k' are colinear.

Proof. It is sufficient to look at the first two eigenvalues of rectangles (which are explicitly known) to conclude that the region $\mathcal{E}_{\mathcal{C}}^D$ is unbounded.
Now let P_1 and P_2 be two arbitrary points in the region $\mathcal{E}_{\mathcal{C}}^D$. By definition of $\mathcal{E}_{\mathcal{C}}^D$, there exist two open planar convex sets with unit area Ω_1 and Ω_2 for which

$$(\lambda_1(\Omega_1), \lambda_2(\Omega_1)) = P_1,\ (\lambda_1(\Omega_2), \lambda_2(\Omega_2)) = P_2.$$

Now let us consider the family of convex domains defined by (Minkowski sum)

$$\Omega_t = t\Omega_1 + (1-t)\Omega_2,\ 0 \le t \le 1.$$

The map $t \mapsto \Omega_t$ is continuous when the set of convex domains is endowed with the Hausdorff convergence (see e.g. [HP] or [G] for more details on this convergence). By continuity of the volume and the Dirichlet eigenvalues for the Hausdorff convergence of convex sets (see Theorem 2.3.17 in [H] for the eigenvalues), the continuous path

$$\{(|\Omega_t|\lambda_1(\Omega_t), |\Omega_t|\lambda_2(\Omega_t),\ t \in [0,1]\}$$

is contained in $\mathcal{E}_{\mathcal{C}}^D$ and connects the points P_1 and P_2. We conclude that $\mathcal{E}_{\mathcal{C}}^D$ is connected by arcs. Now let us prove that the region $\mathcal{E}_{\mathcal{C}}^D$ is closed. Let Ω_n be a sequence of convex domains of area 1 such that $(\lambda_1(\Omega_n), \lambda_2(\Omega_n)) \to (x, y)$. We use the following inequality due to Makai in [M], which holds for any convex planar domains

$$\frac{\pi^2|\partial\Omega|^2}{16|\Omega|^2} \le \lambda_1(\Omega)$$

to claim that the sequence Ω_n has a bounded perimeter. Thus, by translation, we can assume that Ω_n stays in some bounded fixed ball. The Blaschke selection Theorem (see also more generally Corollary 2.2.24 in [HP]) shows that we can extract from the sequence Ω_n a subsequence which converges for the Hausdorff convergence and the result follows using continuity of the eigenvalues for this convergence for convex domains.

Now we will use the Hadamard formula of differentiation with respect to the domain (see eg. [H, HP, SZ]). We recall its definition. Let us consider an open set Ω and an application $\Phi(t)$ such that

$$\Phi : t \in [0, T[\to W^{1,\infty}(\mathbb{R}^N, \mathbb{R}^N) \text{ is differentiable at 0 with } \Phi(0) = I,\ \Phi'(0) = V,$$

where $W^{1,\infty}(\mathbb{R}^N, \mathbb{R}^N)$ is the set of bounded Lipschitz maps from $\mathbb{R}^N$ into itself, I is the identity and V is a deformation field. Let us denote by $\Omega_t = \Phi(t)(\Omega)$, $\lambda_k(t) = \lambda_k(\Omega_t)$ and by u_k a (normalized) eigenfunction of Ω associated to $\lambda_k(0)$ in $H_0^1(\Omega)$. If we assume that Ω is convex and $\lambda_k(\Omega)$ is simple then

$$\lambda_k'(0) = -\int_{\partial\Omega} |\nabla u_k|^2 V.n\, d\sigma. \tag{4}$$

We will also use the formulae for the derivative of the area. Define the function $Area(t) = |\Omega_t|$ then, if Ω is Lipschitz, we have

$$Area'(0) = \int_{\partial\Omega} V.n\, d\sigma. \tag{5}$$

Therefore, if we make the product, by (4) and (5) we have

$$(\lambda_k(\Omega)|\Omega|)'(0) = \lambda_k(0)Area'(0) + \lambda_k'(0)|\Omega| = \int_{\partial\Omega} \left[\lambda_k - |\nabla u_k|^2|\Omega|\right] V.n\, d\sigma. \tag{6}$$

Thus, if we make a deformation of a given convex set Ω through a deformation field V *which preserves convexity*, we define a curve starting from $(x_0, y_0) = (|\Omega|\lambda_1(\Omega), |\Omega|\lambda_2(\Omega))$ with a tangent in the direction of the vector

$$X_V := \left(\int_{\partial\Omega} \left[\lambda_1 - |\nabla u_1|^2|\Omega|\right] V.n\, d\sigma, \int_{\partial\Omega} \left[\lambda_2 - |\nabla u_2|^2|\Omega|\right] V.n\, d\sigma\right)^T. \tag{7}$$

In particular, if we are able to choose deformation fields V such that the vector X_V covers all possible directions, it means that Ω lies in the interior of $\mathcal{E}_{\mathcal{C}}^D$.

Let us consider the strictly convex case. Then, up to first order variations, we can assume that any deformation field V is admissible, in the sense that it preserves convexity, see Theorem 4.2.2 in [H] for more details. Since the map $V \mapsto X_V$ is linear, then either its range is of dimension two (and thus Ω lies in the interior of $\mathcal{E}_{\mathcal{C}}^D$) or its range is of dimension less or equal to one which means:

(8)

$$\exists a, b \in \mathbb{R}, \text{ such that } \forall V, \int_{\partial\Omega} \left[a(\lambda_1 - |\nabla u_1|^2|\Omega|) + b(\lambda_2 - |\nabla u_2|^2|\Omega|)\right] V.n \, d\sigma = 0\,.$$

This implies that the functions $1, |\nabla u_1|^2, |\nabla u_2|^2$ are linearly dependent on the boundary of Ω.

Now, let us consider the case of a polygon with N sides. Obviously, we can perform only a few variations if we want to preserve convexity, see e.g. Theorem 7.5 in [J] or Theorem 4.2.2 in [H] for an analysis of the Hadamard formula for non strictly convex domains in this context. We choose here to move a side γ_k of the polygon

- either in a parallel way (which corresponds to choose a constant deformation field $V.n \equiv 1$ on the side γ_k)
- or to rotate it from one of its vertex (which corresponds to choose a deformation field proportional to the arc-length $V.n \equiv t$ on the side γ_k).

Actually, combination of the previous deformations exactly correspond to move the vertices of the polygon. Each of these deformations preserve convexity and the vectors X_V defined in (7) correspond to the $2N$ vectors V_k and V_k' defined in (3). If these $2N$ vectors were not colinear, we would be able, by linear combination, to make a perturbation of $|\Omega|\lambda_1(\Omega), |\Omega|\lambda_2(\Omega),)$ in any direction proving that the polygon Ω is not on the boundary of $\mathcal{E}_{\mathcal{C}}^D$. $\square$

Remark 2.3. Point 2 of the previous theorem has a local character: if the boundary of a convex set Ω has a part γ which is strictly convex and if Ω is on the boundary of $\mathcal{E}_{\mathcal{C}}^D$, then the linear dependence of $1, |\nabla u_1|^2, |\nabla u_2|^2$ will hold on γ.

Figure 3 seems to suggest that some rectangles are on the lower boundary of $\mathcal{E}_{\mathcal{C}}^D$, but we are going to prove that it is not true. Unfortunately, we cannot use last part of Theorem 2.2. Indeed, if we compute the 8 vectors defined in (3) for the rectangle $(0, L) \times (0, \ell)$, we get 8 vectors colinear to $V = \begin{pmatrix} \frac{\pi^2}{\ell^2} - \frac{\pi^2}{L^2} \\ \frac{\pi^2}{\ell^2} - \frac{4\pi^2}{L^2} \end{pmatrix}$. The reason is the following: the perturbations used in Theorem 2.2 consist in moving the vertices of the polygon. Now, the rectangles are (certainly) on the boundary of the set $\mathcal{E}_{\mathcal{C}}^D$ restricted to quadrilaterals, see Figure 2 and then we need more sophisticated perturbations to prove the following:

Theorem 2.4. *Except for the square, the rectangles are not on the boundary of the region $\mathcal{E}_{\mathcal{C}}^D$.*

Proof. Let $L > 1$ and define a rectangle $\mathcal{R}_L$ (with unit area) by the vertices $(0, 0)$, $(L, 0)$, $(L, 1/L)$ and $(0, 1/L)$. We have

$$\lambda_1 = \pi^2 \left(\frac{1}{L^2} + L^2\right), \ \lambda_2 = \pi^2 \left(\frac{4}{L^2} + L^2\right)$$

and the corresponding normalized eigenfunctions are

$$u_1(x,y) = 2\sin\left(\frac{\pi x}{L}\right)\sin(\pi y L)\,,\ u_2(x,y) = 2\sin\left(\frac{2\pi x}{L}\right)\sin(\pi y L)\,.$$

Now consider a pentagon obtained from the rectangle moving the point $(L, 1/(2L))$ in the direction of the vector $(1,0)$ (see Figure 6) and define

$$\Gamma_1 = \left\{(x,y) : x = L, 0 \le y \le \frac{1}{2L}\right\},\ \Gamma_2 = \left\{(x,y) : x = L, \frac{1}{2L} < y \le \frac{1}{L}\right\}$$

The deformation field is

FIGURE 6. A perturbation of a rectangle.

$$V(x,y) = \begin{cases} (2Ly, 0), & (x,y) \in \Gamma_1 \\ (2-2Ly, 0), & (x,y) \in \Gamma_2. \end{cases} \tag{9}$$

Then, by (6)

$$\left(\lambda_1(\mathcal{R}_L)|\mathcal{R}_L|\right)'(0) =$$
$$\int_0^{\frac{1}{2L}} \left[\lambda_1 - \frac{4\pi^2}{L^2}\sin^2 L\pi y\right] 2Ly dy + \int_{\frac{1}{2L}}^{\frac{1}{L}} \left[\lambda_1 - \frac{4\pi^2}{L^2}\sin^2 L\pi y\right](2-2Ly)dy =$$
$$\frac{L\pi^2}{2} - \left(4 + \frac{\pi^2}{2}\right)\frac{1}{L^3}$$

The calculations for λ_2 are similar leading to

$$\left(\lambda_2(\mathcal{R}_L)|\mathcal{R}_L|\right)'(0) = \frac{L\pi^2}{2} - \left(16 + 2\pi^2\right)\frac{1}{L^3}.$$

Then, for this particular perturbation of the rectangle,

$$\frac{\left(\lambda_2(\mathcal{R}_L)|\mathcal{R}_L|\right)'(0)}{\left(\lambda_1(\mathcal{R}_L)|\mathcal{R}_L|\right)'(0)} = \frac{\frac{L\pi^2}{2} - \left(16+2\pi^2\right)\frac{1}{L^3}}{\frac{L\pi^2}{2} - \left(4+\frac{\pi^2}{2}\right)\frac{1}{L^3}} = \frac{-32 + (L^4-4)\pi^2}{-8 + (L^4-1)\pi^2} := \mathcal{Q}_1(L).$$

On the other hand, for rectangles we have (here ’ denotes the derivative with respect to L)

$$\lambda_1'(L) = \pi^2\left(\frac{-2}{L^3} + 2L\right),\ \lambda_2'(L) = \pi^2\left(\frac{-8}{L^3} + 2L\right)$$

and we shall compare $\mathcal{Q}_1(L)$ with

$$\mathcal{Q}_2(L) := \frac{\lambda_2'(L)}{\lambda_1'(L)} = \frac{\pi^2\left(\frac{-8}{L^3} + 2L\right)}{\pi^2\left(\frac{-2}{L^3} + 2L\right)} = \frac{L^4-4}{L^4-1}.$$

We note that

$$\mathcal{Q}_2(L) = \frac{L^4-1-3}{L^4-1} = 1 - \frac{3}{L^4-1}$$

and

$$\mathcal{Q}_1(L) = \frac{-32 + (L^4-4)\pi^2}{-8+(L^4-1)\pi^2} = \frac{-24-8+(L^4-1)\pi^2-3\pi^2}{-8+(L^4-1)\pi^2} = 1 - \frac{24/\pi^2+3}{-8/\pi^2+L^4-1}.$$

Then,

$$24/\pi^2+3>3,\ -8/\pi^2+L^4-1<L^4-1 \Rightarrow \mathcal{Q}_1(L)<\mathcal{Q}_2(L),\ \forall L>1.$$

and the perturbation that we described above allows the point $(|\Omega|\lambda_1, |\Omega|\lambda_2)$ to go bellow the values obtained for the rectangles. $\square$

To illustrate the result that we proved, in Figure 7 we plot the curve of the rectangles, the unitary vector which is tangent to the curve (in blue) and the unitary vector associated to the perturbation described in the proof of Theorem 2.4 (in red).

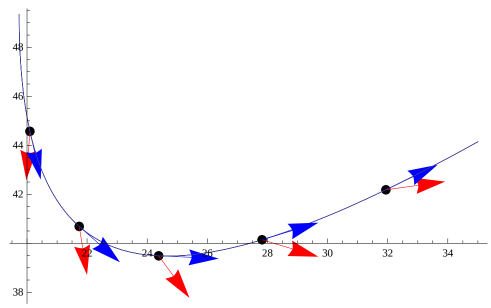

FIGURE 7. The rectangles and the tangent vectors.

Actually, we think that the lower part of the region $\mathcal{E}_{\mathcal{C}}^D$ only contains points corresponding to regular domains and thus not polygons. It can be seen as a question related to the regularity of some shape optimization problem, namely minimizing λ_2 with λ_1 fixed which is out of the scope of this paper. It is a difficult question, see e.g. [B] for similar results. Nevertheless, to prove this claim, we can also consider a similar method to the one used for rectangles. For example, if we could prove that the lower part of $\mathcal{E}_{\mathcal{C}}^D$ is a convex curve $\mathcal{C}$, perturbations which consist in splitting a side in two parts as we did for rectangles would allow to find a continuous curve of perturbations with a tangent (strictly) below $\mathcal{C}$.

Conjecture 4. The lower part of the boundary of $\mathcal{E}_{\mathcal{C}}^D$ does not contain any polygon.

The numerical results showed in Figure 2 suggest that the equilateral triangle and the square are on the upper part of the boundary of the region obtained for quadrilaterals. Thus, it is an interesting question to know which is the tangent to the boundary at those points. Using simple variational methods, it is possible to prove that the tangent at the equilateral triangle is vertical. By (2) we can infer that the tangent at the square is also vertical. For the general case of the region $\mathcal{E}^D$, Wolf and Keller proved in [WK] that the tangent at the ball is vertical. Moreover, if we could prove that the domains minimizing λ_2 with λ_1 fixed are regular, this would prove that these domains are still convex, for λ_1 close to the value for the ball, as regular perturbation of the ball. Therefore, the tangent of the lower part of $\partial\mathcal{E}_{\mathcal{C}}^D$ at the point associated to the ball would be vertical.

As already mentioned, we were not able to prove, but we believe that

Conjecture 5. The region $\mathcal{E}_C^D$ is simply connected.

3. The Neumann case

In this section we consider the similar question of finding the range of the first two non-trivial eigenvalues in the Neumann case. Let $\Omega \subset \mathbb{R}^2$ be a bounded open set. Since we want to restrict ourselves to a discrete spectrum, we will assume that the embedding $H^1(\Omega) \hookrightarrow L^2(\Omega)$ is compact. It is well known that a Lipschitz boundary is a sufficient condition for it to hold. We consider the Neumann eigenvalue problem,

$$\begin{cases} -\Delta u = \mu u & \text{in } \Omega \\ \partial_n u = 0 & \text{on } \partial\Omega, \end{cases} \tag{10}$$

defined on $H^1(\Omega)$. Let us denote the eigenvalues by $0 = \mu_0 \leq \mu_1(\Omega) \leq \mu_2(\Omega) \leq ...$ (counted with their multiplicities) and the corresponding orthonormal real eigenfunctions by $u_0 = 1/\sqrt{|\Omega|}$ and $u_i,\ i = 1, 2, ...$

Remark 3.1. If Ω is disconnected, for example if $\Omega = \cup_{k=1}^N \Omega_k$, where $N \geq 2$ and Ω_k are disjoint bounded connected open sets, we have

$$0 = \mu_0(\Omega) = \mu_1(\Omega) = ... = \mu_{N-1}(\Omega) < \mu_N(\Omega) = min\{\mu_1(\Omega_1), ..., \mu_1(\Omega_N)\},$$

because we can choose an eigenfunction of Ω to be constant in one of the sets Ω_k and vanish in the others. In particular any set Ω which is the union of three disjoint sets satisfies $\mu_1(\Omega) = \mu_2(\Omega) = 0$ and then the corresponding point in $\mathcal{E}^N$ (see below) is the origin.

Our study will focus on the first two (nontrivial) eigenvalues μ_1 and μ_2. We start with the general case of a planar bounded set and then we consider the convex case.

3.1. **General planar bounded sets.** In this section we will study the region

$$\mathcal{E}^N := \left\{(x, y) \in \mathbb{R}^2 : (x, y) = (\mu_1(\Omega), \mu_2(\Omega)),\ \Omega \subset \mathbb{R}^2, |\Omega| = 1\right\}.$$

Some results that are already known help us to plot the corresponding picture. It has been conjectured by Kornhauser and Stakgold in [KS] that the disk maximizes μ_1 among plane domains of given area. This result has been proved by Szegö in [S] for Lipschitz simply connected domains and generalized by Weinberger in [W] to arbitrary (not necessarily simply connected) domains in any dimension. The result can be written as

$$\mu_1(\Omega)|\Omega| \leq \mu_1(\mathcal{B}) \approx 10.64986. \tag{11}$$

Moreover, μ_1 is double at the ball and then the point in $\mathcal{E}^N$ corresponding to the ball is on the line $\mu_2 = \mu_1$. Recently Girouard, Nadirashvili and Polterovich proved in [GNP] that the maximum of μ_2 among simply connected bounded domains is attained for two disjoint balls of equal area, which can be written as

$$\mu_2(\Omega)|\Omega| \leq 2\mu_1(\mathcal{B}) \approx 21.29973. \tag{12}$$

In [S], it has been proved that for simply connected domains with unit area we have

$$\frac{1}{\mu_1(\Omega)} + \frac{1}{\mu_2(\Omega)} \geq \frac{1}{\mu_1(\mathcal{B})} + \frac{1}{\mu_2(\mathcal{B})} \tag{13}$$

which can be written as

$$\mu_2(\Omega) \leq \frac{\mu_1(\Omega)\mu_1(\mathcal{B})}{2\mu_1(\Omega) - \mu_1(\mathcal{B})} := g(\mu_1). \tag{14}$$

These results and the trivial bounds $\mu_2 \geq \mu_1$ and $\mu_1 \geq 0$ allow to plot a region (Figure 8) which contains $\mathcal{E}^N$ (at least if we restrict ourselves to simply connected domains). Now we will concern our study in knowing which part of the region of

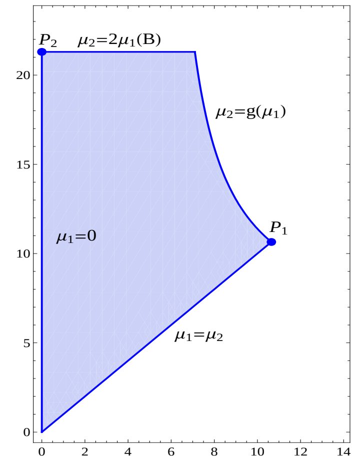

FIGURE 8. A region generated by the bounds for μ_1 and μ_2 which contains $\mathcal{E}^N$.

Figure 8 is contained in $\mathcal{E}^N$. We denote by $\alpha\Omega$ the image of Ω by an homothety with ratio $\alpha > 0$ and start proving an auxiliary result.

Lemma 3.2. *Let Ω_1^* and Ω_2^* be two open connected disjoint sets with $|\Omega_1^*| = |\Omega_2^*| = 1$. Define $m = min\,(\mu_1(\Omega_1^*), \mu_1(\Omega_2^*))$ and for each $A \in]0, 1[$ let Ω be the domain $\Omega = \left(\sqrt{A}\,\Omega_1^*\right) \cup \left(\sqrt{1-A}\,\Omega_2^*\right)$. Then,*

$$\{(\mu_1(\Omega), \mu_2(\Omega)),\ A \in]0, 1[\} = \{0\} \times]m, \mu_1(\Omega_1^*) + \mu_1(\Omega_2^*)].$$

Moreover, the maximum of $\mu_2(\Omega)$ among all possible values $A \in]0, 1[$ is attained when $A = A^* := \frac{\mu_1(\Omega_1^*)}{\mu_1(\Omega_1^*)+\mu_1(\Omega_2^*)}$.

Proof. We know that $|\alpha\Omega| = \alpha^2|\Omega|$, then $|\Omega| = A|\Omega_1^*| + (1-A)|\Omega_2^*| = 1$. Now $0 < A < 1 \Rightarrow 0 < \sqrt{1-A} < 1$, and then both components does not degenerate into a single point and Ω has exactly two disjoint components. By Remark 3.1, we have $\mu_1(\Omega) = 0$ and $\mu_2(\Omega) = min(\mu_1(\sqrt{A}\Omega_1^*), \mu_1(\sqrt{1-A}\Omega_2^*))$. Thus

$$\mu_2(\Omega) = \min\left(\frac{\mu_1(\Omega_1^*)}{A}, \frac{\mu_1(\Omega_2^*)}{1-A}\right) = \begin{cases} \frac{\mu_1(\Omega_2^*)}{1-A} & \text{if } A \leq A^* \\ \frac{\mu_1(\Omega_1^*)}{A} & \text{if } A \geq A^* \end{cases}$$

and the Lemma follows. $\square$

Remark 3.3. By Lemma 3.2 and inequality (11) it is easy to conclude that the maximum of μ_2 among all disconnected sets Ω is attained for two balls with the same area, which is a much weaker result but related with inequality (12).

We will also need three classical results, the first one related to symmetry and multiplicity, the second one to symmetry and the third one to continuity of eigenvalues. The first Lemma is due to M. Ashbaugh and R. Benguria in [AB3, Lemma 4.1]:

Lemma 3.4. *If $\Omega \subset \mathbb{R}^2$ is a simply connected domain with k-fold symmetry where $k \geq 3$, then $\mu_2 = \mu_1$.*

The second lemma is classical, but we give a proof here for sake of completeness.

Lemma 3.5. *If $\Omega \subset \mathbb{R}^N$ is symmetric with respect to some hyperplane H, then for each eigenvalue we can find an eigenfunction which is either even or odd with respect to H.*

Proof. Let x' denotes the reflection of x with respect to H. Obviously, if $v(x)$ is an eigenfunction (Dirichlet or Neumann) associated to an eigenvalue λ, the function $w(x) := v(x')$ is still an eigenfunction associated to λ and it has the same L^2 norm. Therefore the case of a simple eigenvalue is clear since we have then $w = v$ (v even) or $w = -v$ (v odd).

Let us now consider the case of a multiple eigenvalue. Let $v_1, v_2, \ldots, v_m$ be an orthogonal sequence of eigenvalues spanning the eigenspace V. For each k, the function $w_k(x) := v_k(x')$ is in V. Let A be the linear transformation mapping the v_k onto the w_k. Since $x'' = x$, the map A is an involution: $A^2 = Id$. Thus $\det(A^2 - Id) = \det(A - Id). \det(A + Id) = 0$ and 1 or -1 is an eigenvalue of A. Now, we look for a combination of the v_k: $w = \sum_k \alpha_k v_k$ such that $w(x') = w(x)$ or $w(x') = -w(x)$. This exactly corresponds to looking for an eigenvector of A associated to the eigenvalue 1 or -1 which is always possible. $\square$

Remark 3.6. If Ω has two axis of symmetry and if we are interested in the second or third eigenvalue, a simple consequence is that there exists an eigenfunction which is even with respect to one of the axis of symmetry. Indeed, according to Cayley-Hamilton Theorem, the minimal polynomial of A divides its characteristic polynomial. Now, this minimal polynomial is either X^2-1, or $X-1$ or $X+1$. Thus the only case where we could not find an even eigenfunction would be if the minimal polynomial is $X+1$ for both reflections with respect to the two hyperplane. Now, it would imply that the eigenfunctions are odd with respect to the two hyperplane. But this would imply that the eigenfunctions have (at least) four nodal domains.

The third Lemma is mainly due to D. Chenais in [C], see also [H, Theorem 2.3.25] and [HP, Theorem 3.7.2].

Lemma 3.7. *Let B be a fixed compact set in $\mathbb{R}^N$ and Ω_n a sequence of open subsets of B. Assume that the sets Ω_n are* **uniformly Lipschitz** *(in the sense that there exists a uniform Lipschitz constant for all the domains in the sequence). Assume moreover that Ω_n converge, for the Hausdorff distance, to Ω. Then, for every fixed k, $\mu_k(\Omega_n) \to \mu_k(\Omega)$.*

Remark 3.8. More generally, the previous continuity property holds true if we can find a sequence of extension operators $P_n : H^1(\Omega_n) \mapsto H^1(B)$ with $\|P_n\|$ (the operator norm) uniformly bounded.

Denote by O the origin and define the points $P_1 = (\mu_1(\mathcal{B}), \mu_2(\mathcal{B})) \approx (10.649, 10.649)$ and $P_2 = (0, 2\mu_1(\mathcal{B})) \approx (0, 21.29973)$ see Figure 8. In the region $\mathcal{E}^N$, these points correspond to the ball and two identical balls respectively. Now we define the paths

$$\Gamma_{O,P_1} = \{(t,t) : t \in [0, \mu_1(\mathcal{B})]\}$$

and

$$\Gamma_{O,P_2} = \{(0,t) : t \in [0, 2\mu_1(\mathcal{B})]\}$$

and prove that these paths are contained in the region $\mathcal{E}^N$. We gather in the next theorem, the main theoretical results we are able to prove concerning $\mathcal{E}^N$

Theorem 3.9. *We have $\Gamma_{O,P_1} \subset \mathcal{E}^N$ and $\Gamma_{O,P_2} \subset \mathcal{E}^N$. More precisely, the region $\mathcal{E}^N$ contains the following sub-domains (see Figure 11)*

$$\Gamma_{1,L} := \left\{ \left(t, \frac{4\pi^2}{L^2}\right) : t \in \left[0, \frac{\pi^2}{L^2}\right] \right\}, \forall L \in [\sqrt{2}, \infty[,$$

$$\Gamma_{2,L} := \left\{ \left(t, \pi^2 L^2\right) : t \in \left[0, \frac{\pi^2}{L^2}\right] \right\}, \forall L \in [1, \sqrt{2}]$$

and

$$\Gamma_3 := \{(x,y) : 0 < x \le y \le \mu_1(\mathcal{B})\}.$$

At last, the tangent of the boundary of $\mathcal{E}^N$ at the point P_1 is parallel to the second bisectrix $y + x = 0$.

Proof. We have $O \in \mathcal{E}^N$ (see Remark 3.1). Now let Ω_a, $a < 1/2$ be the polygonal domain plotted in Figure 9, which is the union of two rectangles with length sides equal to 2 and $2a$. For these domains, according to Lemma 3.4 we have that

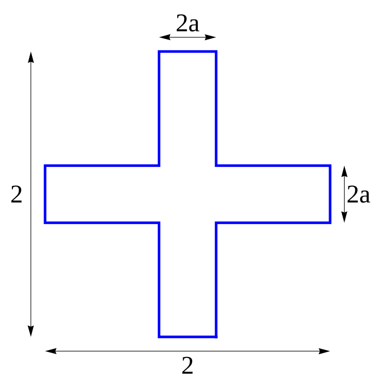

FIGURE 9. Polygonal domain Ω_a associated to the path Γ_{O,P_1}.

$\mu_2 = \mu_1$, because of the 4-fold symmetry. Now we prove that

$$\mu_1(\Omega_a)|\Omega_a| \to 0, \text{ when } a \to 0.$$

We know that

$$\mu_1(\Omega_a) = \inf_{v \in H^1(\Omega_a), v \neq 0, \int_{\Omega_a} v = 0} \frac{\int_{\Omega_a} |\nabla v(x)|^2 dx}{\int_{\Omega_a} v(x)^2 dx}$$

and then

$$\mu_1(\Omega_a) \le \frac{\int_{\Omega_a} |\nabla v(x)|^2 dx}{\int_{\Omega_a} v(x)^2 dx}$$

where v is the test function

$$v(x,y) = \cos\left(\frac{\pi(x-1)}{2}\right)$$

that satisfies $\int_{\Omega_a} v = 0$. Now we have

$$\int_{\Omega} v^2 dx = 4a - \frac{2\sin(a\pi)}{\pi} - 2a^2 + \frac{2a\sin(a\pi)}{\pi}$$

and

$$\int_{\Omega} |\nabla v|^2 dx = a\pi^2 + \frac{\pi\sin(a\pi)}{2} - \frac{a^2\pi^2}{2} - \frac{a\pi\sin(a\pi)}{2}.$$

Then, using $\sin\pi a \leq \pi a$, we get

$$\mu_1(\Omega_a) \leq \frac{\int_\Omega |\nabla v|^2 dx}{\int_\Omega v^2 dx} \leq \frac{a\pi^2 + \pi^2 a/2}{4a - 2a - 2a^2} \leq \frac{3\pi^2}{2}.$$

Now, we have $|\Omega_a| = 8a - 4a^2$ and therefore

$$\mu_2(\Omega_a)|\Omega_a| \to 0,\ a \to 0.$$

Let us fix $a' = \frac{1}{2}$. By continuity of the Neumann eigenvalues (apply Lemma 3.7) we have

$$\{(|\Omega_a|\mu_1(\Omega_a), |\Omega_a|\mu_2(\Omega_a)), a \in]0, a']\} = \{(t,t), t \in]0, \mu_1(\Omega_{a'})]\}.$$

Now for $t \in [0,1[$, let Ω^t be the domain defined by $\Omega^t = (1-t)\Omega_{a'} + t\mathcal{B}$ which has the same type of symmetries of Ω_a, and then we have $\mu_2(\Omega^t) = \mu_1(\Omega^t)$ and again by continuity, we have

$$\left\{(\mu_1(\Omega^t), \mu_2(\Omega^t)), t \in [0,1[\right\} = \{(t,t), t \in [\mu_1(\Omega_{a'}), \mu_1(\mathcal{B})[\}.$$

Then we have proved that $\Gamma_{O,P_1} \subset \mathcal{E}^N$. Now we prove that $\Gamma_{O,P_2} \subset \mathcal{E}^N$ using Lemma 3.2 twice. Let $\Omega_1^* = \Omega_2^* = \mathcal{B}$ and Ω be the domain defined in Lemma 3.2. We have $m = min\,(\mu_1(\Omega_1^*), \mu_1(\Omega_2^*)) = \mu_1(\Omega_1^*)$ and then

$$\{(\mu_1(\Omega), \mu_2(\Omega)),\ A \in]0,1[\} = \{0\} \times]\mu_1(\mathcal{B}), 2\mu_1(\mathcal{B})]. \tag{15}$$

Now take $\Omega_1^* = \mathcal{B}$ and $\Omega_2^* = R_L$, where R_L is a rectangle with unit area and whose length sides are $L \geq 1$ and $1/L$. We know that

$$\mu_1(R_L) = \frac{\pi^2}{L^2} \to 0,\ \text{as } L \to \infty.$$

If Ω is the domain defined in Lemma 3.2 we have

$$m = min\,(\mu_1(\Omega_1^*), \mu_1(\Omega_2^*)) = \mu_1(R_L) = \frac{\pi^2}{L^2}$$

and then

$$\{(\mu_1(\Omega), \mu_2(\Omega)),\ A \in]0,1[\} = \{0\} \times \left]\frac{\pi^2}{L^2}, \frac{\pi^2}{L^2} + \mu_1(\mathcal{B})\right]. \tag{16}$$

Now, by (15) and (16) and taking $L \to \infty$, we conclude that

$$\{0\} \times]0, 2\mu_1(\mathcal{B})] \subset \mathcal{E}^N$$

and we get the conclusion.

Now we prove that we have x-convexity in some parts of the region $\mathcal{E}^N$. Let $\mathcal{R}_L$ be a rectangle with unit area for which the length of the largest side is equal to L. We will assume that the vertices are the points $(0,0)$, $(L,0)$, $(L,1/L)$ and $(0,1/L)$.

If we have $L \in [\sqrt{2}, \infty[$, then $\mu_1(\mathcal{R}_L) = \frac{\pi^2}{L^2}$ and $\mu_2(\mathcal{R}_L) = \frac{4\pi^2}{L^2}$. The associated eigenfunctions are

$$u_1(x,y) = \sqrt{2}\cos\left(\frac{\pi x}{L}\right) \quad u_2(x,y) = \sqrt{2}\cos\left(\frac{2\pi x}{L}\right). \tag{17}$$

In the case $L = \sqrt{2}$ we have $\mu_2(\mathcal{R}_L) = \mu_3(\mathcal{R}_L)$ and u_2 given by (17) is one of the possible eigenfunctions associated to μ_2. Now we note that

$$\frac{\partial u_2}{\partial x}(x,y) = -\frac{2\pi}{L}\sin\left(\frac{2\pi x}{L}\right) \Rightarrow \frac{\partial u_2}{\partial x}\left(\frac{L}{2}, y\right) = 0.$$

Let us introduce the domain $\mathcal{R}_{L,\alpha}$ plotted in Figure 10 corresponding to the previous rectangle where we remove two segments of length α at $x = L/2$. We can check that the embedding $H^1(\mathcal{R}_{L,\alpha}) \hookrightarrow L^2(\mathcal{R}_{L,\alpha})$ is still compact. Indeed it is possible to make two reflections along the axis of symmetry for any function in $H^1(\mathcal{R}_{L,\alpha})$ and we easily get compactness in L^2 of any bounded sequence. Thus the spectrum of the Neumann-Laplacian on $\mathcal{R}_{L,\alpha}$ is discrete. Moreover, for $0 < \alpha < \alpha' < 1/2L$, we have

$$H^1(\mathcal{R}_L) \hookrightarrow H^1(\mathcal{R}_{L,\alpha}) \hookrightarrow H^1(\mathcal{R}_{L,\alpha'}) \hookrightarrow H^1(\mathcal{R}_{L,1/2L})$$

therefore, by the min-max formulae, for any eigenvalue

$$\mu_k(\mathcal{R}_{L,1/2L}) \leq \mu_k(\mathcal{R}_{L,\alpha'}) \leq \mu_k(\mathcal{R}_{L,\alpha}) \leq \mu_k(\mathcal{R}_L). \tag{18}$$

Now $\mathcal{R}_{L,1/2L}$ is the union of two disjoint rectangles and $\mu_1(\mathcal{R}_{L,1/2L}) = \mu_2(\mathcal{R}_{L,1/2L}) = \mu_2(\mathcal{R}_L)$ (the corresponding eigenfunction being u_2 defined in (17)). Therefore, in (18) we have for any α, $\mu_2(\mathcal{R}_{L,\alpha}) \leq \mu_2(\mathcal{R}_L)$. Moreover, $\mu_1(\mathcal{R}_{L,\alpha})$ decreases continuously from $\mu_1(\mathcal{R}_L)$ to 0 (use Remark 3.8 for the continuity). Then we conclude that

$$\mathcal{E}^N \supset \Gamma_{1,L} := \left\{\left(t, \frac{4\pi^2}{L^2}\right) : t \in \left[0, \frac{\pi^2}{L^2}\right]\right\}, \forall L \in [\sqrt{2}, \infty[.$$

The same analysis is valid in the case $L \in [1, \sqrt{2}]$ and allows to prove that

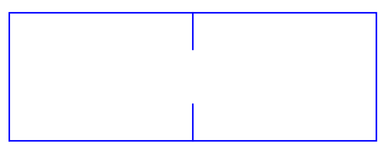

FIGURE 10. Perturbation of $\mathcal{R}_L$ which preserves μ_2 and decreases μ_1.

$$\mathcal{E}^N \supset \Gamma_{2,L} := \left\{\left(t, \pi^2 L^2\right) : t \in \left[0, \frac{\pi^2}{L^2}\right]\right\}, \forall L \in [1, \sqrt{2}].$$

Thus, we conclude that the region plotted in Figure 11-left is contained in $\mathcal{E}^N$. The curve corresponding to the rectangles is also plotted in the Figure.

Now we note that the same argument can be applied for the family of domains with 4-fold symmetry and two axes of symmetry (which corresponds to points on the first diagonal $\mu_1 = \mu_2$) such as the domain plotted in Figure 9. Let Ω be such a domain which satisfies $\mu_2(\Omega) = \mu_1(\Omega)$. According to Lemma 3.5 and Remark 3.6, we know that there exists one eigenfunction associated to $\mu_1(\Omega_t)$ which satisfies a null Neumann condition on the axis of symmetry. Then, we can add two segments on that line and we conclude that, when we increase the length of the segments, one of the eigenvalues goes to zero, and the other remain constant. The only point that we need to check here is that the second eigenvalue of the disconnected domain is still $\mu_2(\Omega)$. Actually, if there would exist an eigenfunction with a smaller eigenvalue on half of the domain, we would be able, by reflection, to construct an eigenfunction on Ω with the same eigenvalue, which is impossible. Then we proved that

$$\mathcal{E}^N \supset \Gamma_3 := \{(x,y) : 0 < x \leq y \leq \mu_1(\mathcal{B})\}\,.$$

Joining this regions and the result of Theorem 3.9 we have proved that the region plotted in Figure 11-right is contained in $\mathcal{E}^N$.

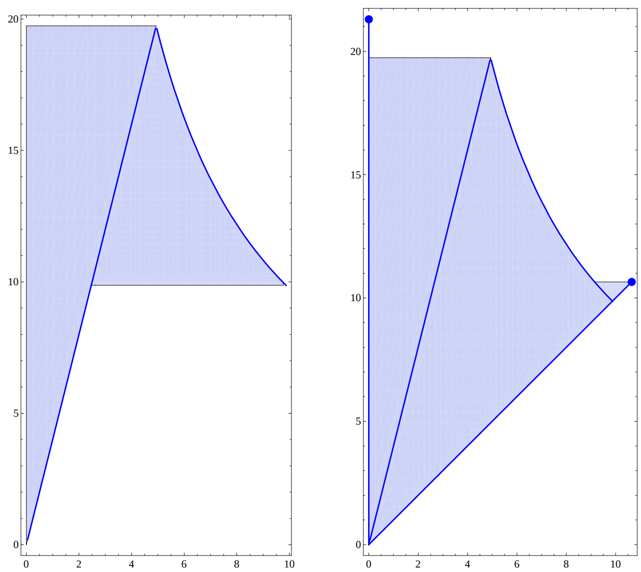

FIGURE 11. Regions which are contained in $\mathcal{E}^N$.

Now we study the tangent of $\mathcal{E}^N$ at the point P_1 which corresponds to the ball. By (14) and writing $c = \mu_1(\mathcal{B})$ we have

$$\mu_2'(\mu_1) \leq g'(\mu_1) = \frac{c(2\mu_1 - c) - 2c\mu_1}{(2\mu_1 - c)^2} = \frac{-c^2}{(2\mu_1 - c)^2} \Rightarrow \mu_2'(\mu_1(\mathcal{B})) \leq \frac{-c^2}{(2c - c)^2} = -1. \tag{19}$$

Now to prove that the line $x + y = 2\mu_1(\mathcal{B})$ is the tangent line at P_1, it remains to exhibit a deformation of the ball which has this behavior. For that purpose, we still use the Hadamard formula of derivation with respect to the domain. Now we have to work for Neumann eigenvalues and in the case of a **double** eigenvalue. We keep notations introduced in the proof of Theorem 2.2. If a Neumann eigenvalue is simple, its derivative is given by (see [H, HP]):

$$d\mu_k(\Omega, V) = \int_{\partial\Omega} \left((|\nabla u_k|^2 - \mu_k u_k^2) \right) V.n \, d\sigma\,. \tag{20}$$

Now when we deal with a double eigenvalue, it can be proved (see [H, R]) that μ_1 and μ_2 are not differentiable, but nevertheless $V \mapsto (\mu_1(\Omega_t), \mu_2(\Omega_t))$ has directional derivatives which are precisely the two eigenvalues of the 2×2 matrix $\mathcal{M}$ defined

by (here u_1, u_2 are two normalized orthogonal eigenfunctions):
(21)

$$\mathcal{M} = \left(\begin{array}{cc} \int_{\partial\Omega} \left((|\nabla u_1|^2 - \mu_1 u_1^2)\right) V.n\, d\sigma & \int_{\partial\Omega} ((\nabla u_1.\nabla u_2 - \mu_1 u_1 u_2))\, V.n\, d\sigma \\ \int_{\partial\Omega} ((\nabla u_1.\nabla u_2 - \mu_1 u_1 u_2))\, V.n\, d\sigma & \int_{\partial\Omega} \left((|\nabla u_2|^2 - \mu_1 u_2^2)\right) V.n\, d\sigma \end{array} \right).$$

In the case of the ball where $u_1(r,\theta) = c_1 J_1(\omega r)\cos\theta$ and $u_2(r,\theta) = c_1 J_1(\omega r)\sin\theta$ with $\mu_1 = \mu_2 = \omega^2$, we get
(22)

$$\mathcal{M} = c_1^2 \left(\begin{array}{cc} \int_0^{2\pi} \left(\sin^2\theta - \omega^2\cos^2\theta\right) V.n\, d\theta & -(1+\omega^2)\int_0^{2\pi} \sin\theta\cos\theta\, V.n\, d\theta \\ -(1+\omega^2)\int_0^{2\pi} \sin\theta\cos\theta\, V.n\, d\theta & \int_0^{2\pi} \left(\cos^2\theta - \omega^2\sin^2\theta\right) V.n\, d\theta\ . \end{array} \right)$$

For example, if we choose a deformation of the disk such that $V.n = \cos(2\theta)$, the area is preserved (at first order) and the matrix $\mathcal{M}$ becomes diagonal with eigenvalues $\pm\frac{c_1^2(1+\omega^2)\pi}{2}$. This shows that, for this perturbation, $(\mu_1(\Omega_t), \mu_2(\Omega_t))$ converge to $(\mu_1(\mathcal{B}), \mu_2(\mathcal{B}))$ with the tangent line $x + y = 2\mu_1(\mathcal{B})$. □

To study the tangent at the point P_2 corresponding to two balls with the same area, we can consider a family of domains which are the union of two balls with the same area and a small intersection of size τ. In the limit case $\tau \to 0$, the domain Ω_τ degenerates to two disjoint balls. A numerical study seems to show that this family of domains satisfies: the curve $\tau \mapsto (\mu_1(\Omega_\tau)|\Omega_\tau|, \mu_2(\Omega_\tau)|\Omega_\tau|)$ has an horizontal tangent at $\tau = 0$. This suggests

Conjecture 6. Prove that the tangent of the boundary $\partial\mathcal{E}^N$ at the point P_2 corresponding to two balls, is horizontal.

Finally, we calculated numerically some points on part of the boundary, $\partial\mathcal{E}^N$ which lies between the points corresponding to the ball and two balls. Joining the points that we gathered we are able to plot the region $\mathcal{E}^N$, see Figure 12. All the domains that we found numerically on that part of the boundary have two axes of symmetry.

Conjecture 7. Prove that the domains corresponding to points lying on the "free" boundary of $\mathcal{E}^N$ have two axes of symmetry. If this is the case, following the same argument as in the proof of Theorem 3.9, we could prove that the set $\mathcal{E}^N$ is convex in the x-direction.

3.2. **Convex domains.** In this section we are interested in the study of the region

$$\mathcal{E}_{\mathcal{C}}^N := \left\{(x,y) \in \mathbb{R}^2 : (x,y) = (\mu_1(\Omega), \mu_2(\Omega)),\ |\Omega| = 1,\ \Omega \text{ convex}\right\}.$$

We start presenting some numerical results obtained for polygons.

3.3. **The case of polygons.** In this section we analyze some numerical results that we gathered. We calculated the first two nontrivial Neumann eigenvalues of 3000 triangles, 7800 convex quadrilaterals and 12000 octagons. In Figure 13-left we show the results for triangles. Like in the Dirichlet case, the isosceles triangles seem to be on the boundary of the region for triangles but the superequilateral and subequilateral switch their role. In the Neumann case, the superequilateral define the lower part of the boundary while the subequilateral define the upper boundary. In Figure 13-right we plot results for convex quadrilaterals. The points marked in yellow are obtained by rhomboidal domains and the points in gray correspond to the rectangles. Our numerical results suggest that the rectangles are on the boundary of the region that we obtain for convex quadrilaterals. Actually it is a much more

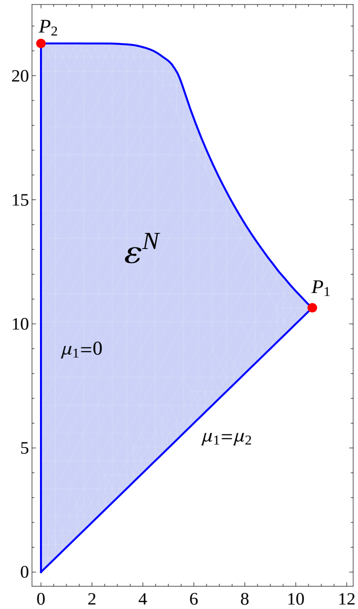

FIGURE 12. The region $\mathcal{E}^N$.

general property which is conjectured, see Conjecture 8 below: the rectangles (for $L \geq 2\ell$) seem to be on the boundary of $\mathcal{E}^N_{\mathcal{C}}$.

Numerically, we observe that the lower part of the boundary (in the case of quadrilaterals) is composed of two different arcs. Denote by T^r the equilateral triangle with unit area. For $\mu_1 \leq \mu_1(T^r) = \frac{4\pi^2}{3\sqrt{3}}$, the lower boundary is defined by the superequilateral triangles and for $\mu_1 \geq \mu_1(T^r)$ the boundary coincides with a segment of quadrilaterals, for which $\mu_1 = \mu_2$, joining the points of the equilateral triangle and the square. In section 3.4, we will prove this last point. In Figure 14 we plot the results obtained for convex octagons. The points corresponding to the regular polygons are marked with larger red points and the ball is represented with a larger black point. We also plotted in blue the upper part of the boundary of the region $\mathcal{E}^N_{\mathcal{C}}$ that was calculated numerically. Note that, as claimed in Conjecture 8, rectangles seem to be on the upper boundary. We will prove a partial result in this direction in section 3.4. In both plots of Figures 13 and 14 we can observe that in each case, μ_1 is maximized (among polygons with a given number of sides) by the regular polygon. This result was proved in the case of triangles in [LS2] but to our knowledge it is an open problem for the other classes of polygons. It is a similar conjecture to Polya's problem for the Dirichlet case as mentioned in [H, section 3.3.3]. We calculated numerically the convex domain that maximizes μ_2 (with unit area) and for the optimizer we obtained $\mu_2 \approx 20.102$. We prove in Theorem 3.11 below that the maximizer is not a stadium. In Figure 15 we plot a superposition of the plots of the convex domain that minimizes λ_2 (dashed red line) and the convex domain which maximizes μ_2 (blue line).

3.4. **Some analytic results.** In this section we shall present some mathematical results for the characterization of the region $\mathcal{E}^N_{\mathcal{C}}$. Define $P_3 = (\mu_1(\mathcal{B}), \mu_2(\mathcal{B})) =$

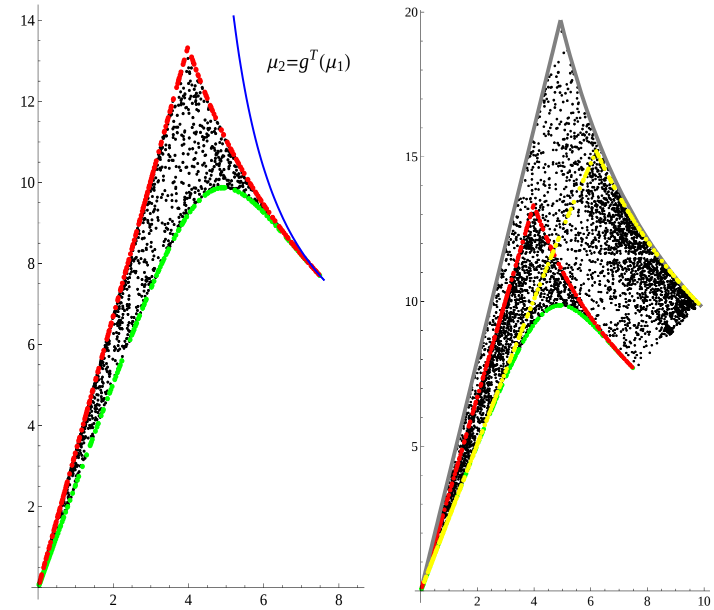

FIGURE 13. The range of the first two Neumann eigenvalues for triangles (left) and convex quadrilaterals (right).

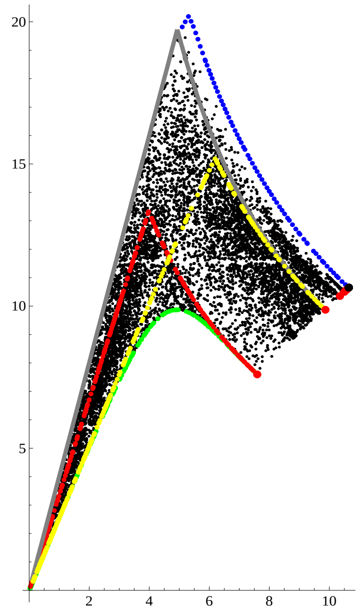

FIGURE 14. The range of the first two non trivial Neumann eigenvalues for octagons.

$(\mu_1(\mathcal{B}), \mu_1(\mathcal{B}))$, $P_4 = (\mu_1(T^r), \mu_2(T^r)) = (\mu_1(T^r), \mu_1(T^r))$ (where T^r is the equilateral triangle) and the segment

$$\Gamma_{P_3,P_4} = \{(t,t) : t \in [\mu_1(T^r), \mu_1(\mathcal{B})]\}\,.$$

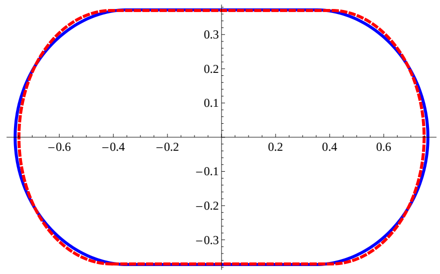

FIGURE 15. The convex optimizers for λ_2 (dashed red line) and μ_2 (blue line).

Theorem 3.10. *The set $\mathcal{E}_{\mathcal{C}}^N$ is not closed. It contains the segment Γ_{P_3,P_4}.*

Proof. Considering a sequence of rectangles $\Omega_n = (0,n) \times (0,1/n)$ we see that $\mu_1(\Omega_n) = \pi^2/n^2$ and $\mu_2(\Omega_n) = 4\pi^2/n^2$. Thus the corresponding point in $\mathcal{E}_{\mathcal{C}}^N$ converges to the origin which is not a point in $\mathcal{E}_{\mathcal{C}}^N$, thus this set is not closed.

For the segment Γ_{P_3,P_4}, the argument is similar to those used in the proof of Theorem 3.9. Let $\Omega_t = t\mathcal{B} + (1-t)T^r$, for $t \in [0,1]$ which defines a family of convex domains. Since Lemma 3.7 applies here, we have continuity of the Neumann eigenvalues. Thus the domains Ω_t define a continuous path connecting the points P_3 and P_4, which by definition, is contained in the region $\mathcal{E}_{\mathcal{C}}^N$. Now due to the symmetries of the domains Ω_t we have $\mu_1(\Omega_t) = \mu_2(\Omega_t)$ (cf. Lemma 3.5) and we get the conclusion. ☐

We have seen in section 3.1 that the maximizer of μ_2 among domains with fixed area is the set composed of two identical balls. Therefore, when we add a convexity constraint, we can wonder whether the maximizer would be the *convex hull* of these two balls, namely a *stadium*. The theorem below shows that it is not the case. This question was already investigated in the Dirichlet case in [HO1] and the answer was also negative. The technique of proof here is similar, though a little bit more complicated.

Theorem 3.11. *The convex domain Ω which maximizes μ_2 (among convex domains with given area) is not a stadium (convex hull of two identical balls). More precisely its boundary does not contain any arc of circle.*

Proof. First of all, it is not difficult to prove the existence of a convex domain Ω of area 1 which maximizes the second Neumann eigenvalue (by the standard method of calculus of variations). Let us denote by u a (normalized) eigenfunction associated to μ_2. Let us assume, for a contradiction, that the boundary of Ω contains an arc of circle γ. We choose the center of coordinates at the center of the circle containing γ.

Using the method of proof of [H, Lemma 2.5.9] or [HO1, Theorem 5], it is possible to prove that the eigenvalue μ_2 is simple. Therefore μ_2 is differentiable under smooth perturbations of γ and since we have a volume constraint, Hadamard formula (20) yields

$$|\nabla u|^2 - \mu_2 u^2 = \text{const} = c \text{ on } \gamma. \tag{23}$$

Let θ denotes the polar angle. We also introduce the operator A_θ defined as

$$A_\theta v := x\frac{\partial v}{\partial y} - y\frac{\partial v}{\partial x}\,.$$

It is classical that A_θ commutes with the Laplacian (and also with the derivative with respect to r). On γ, we have $A_\theta v = v_\theta$ where the subscript θ denotes the derivative with respect to θ.

Due to the Neumann condition $\partial u/\partial n = 0$ on γ, we have $|\nabla u|^2 = u_\theta^2$ on γ. Differentiating with respect to θ equation (23) gives $u_\theta(u_{\theta\theta} - \mu_2 u) = 0$. Let us prove that u_θ cannot be identically 0 on γ (or a part of γ). If it was the case, the function $v := A_\theta u$ would satisfy

$$\begin{cases} -\Delta v = \mu_2 v & \text{in } \Omega \\ v = 0 & \text{on } \gamma \\ \frac{\partial v}{\partial n} = 0 & \text{on } \gamma \end{cases}$$

and therefore, by Hölmgren uniqueness Theorem, we would have v identically 0 in a neighborhood of γ and then in Ω by analyticity. This would imply that u is radially symmetric and that Ω is a disk which cannot be true. Thus, since u_θ is not zero, we have

$$u_{\theta\theta} - \mu_2 u = 0 \quad \text{on } \gamma. \tag{24}$$

We now introduce the function w defined by $w = \mu_2 u + A_\theta^2 u$. By direct computation and (24), we have that w satisfies

$$\begin{cases} -\Delta w = \mu_2 w & \text{in } \Omega \\ w = 0 & \text{on } \gamma \\ \frac{\partial w}{\partial n} = 0 & \text{on } \gamma \end{cases}.$$

Therefore, by Hölmgren uniqueness Theorem, the function w is identically 0 in a neighborhood of γ and then in Ω by analyticity. The fact that u satisfies $u_{\theta\theta} - \mu_2 u = 0$ on each circle centered at the origin implies that u can be written

$$u(r,\theta) = A_1(r)\cos\sqrt{\mu_2}\theta + A_2(r)\sin\sqrt{\mu_2}\theta\,. \tag{25}$$

Now if we plug the expression (25) into $\Delta u + \mu_2 u = 0$, we get $A_j(r) = \alpha_j J_1(\sqrt{\mu_2}r),\ j = 1,2$ where J_1 is the usual Bessel function. Thus to get a contradiction, it suffices to prove the following property:

$$\left.\begin{array}{lr} u = J_1(\sqrt{\mu_2}r)[\alpha_1\cos\sqrt{\mu_2}\theta + \alpha_2\sin\sqrt{\mu_2}\theta] & \text{in } \Omega \\ \frac{\partial u}{\partial n} = 0 & \text{on } \partial\Omega \end{array}\right\} \Longrightarrow \Omega \text{ is a disk.} \tag{26}$$

Now if we write the boundary of Ω (locally) in polar coordinates $\rho = f(\theta)$, the property $\frac{\partial u}{\partial n} = 0$ reads

$$f(\theta)J_1'(\sqrt{\mu_2}f(\theta))[\alpha_1\cos\sqrt{\mu_2}\theta + \alpha_2\sin\sqrt{\mu_2}\theta] - \frac{f'(\theta)}{f(\theta)}[-\alpha_1\sin\sqrt{\mu_2}\theta + \alpha_2\cos\sqrt{\mu_2}\theta] = 0\,. \tag{27}$$

The differential equation (27) can be written $f'(\theta) = F(\theta, f(\theta))$ with $f(\theta_0) = R_0$ (the radius of γ) with F a Lipschitz function. Then this differential equation has a unique solution, but it is clear that $f(\theta) = R_0$ is a solution, so (26) follows and the result is proved. $\square$

We recall the following conjecture already quoted in [AB3]

Conjecture 8. For any convex domain Ω prove that

$$\mu_2(\Omega) \leq 4\mu_1(\Omega). \tag{28}$$

Equality holds if Ω is a rectangle with length L and width ℓ satisfy $L \geq 2\ell$.

Here is a partial result which supports this conjecture.

Proposition 3.12. *For any convex perturbation Ω_t of a rectangle $\Omega = (0, L)\times(0, \ell)$ with $L > 2\ell$, we have $\mu_2(\Omega_t) \leq 4\mu_1(\Omega_t)$.*
In other words, these rectangles are local maximizers of the ratio $\mu_2/4\mu_1$ among convex sets.

Proof. By superposition, it suffices to consider a convex perturbation of $\Omega = (0, L) \times (0, \ell)$ which acts only on the lower side $(0, L) \times \{0\}$. We denote by $v(x) = V.n$ the normal displacement of the point of abscissa $x \in (0, L)$ and to preserve convexity, we assume the function v to be concave. Without loss of generality, we can also assume v to be C^2.

Let us write the first derivative (Hadamard formula) of $|\Omega|(\mu_2(\Omega)-4\mu_1(\Omega))$ using (20) and (5), denoting by D this derivative, and using $u_1 = \sqrt{2}\cos(\pi x/L), \mu_1 = \pi^2/L^2, u_2 = \sqrt{2}\cos(2\pi x/L), \mu_2 = 4\pi^2/L^2$, we get

$$D = \frac{8\pi^2}{L^2}\int_0^L (\cos\frac{2\pi x}{L} - \cos\frac{2\pi x}{L})v(x)\,dx. \tag{29}$$

Integrating D twice by parts and replacing x by $tL/2\pi$ yields

$$D = \frac{8\pi^2}{L^2}\int_0^{2\pi} (\frac{3}{4} - \cos t + \frac{\cos 2t}{4})v''(t)\,dt. \tag{30}$$

Now an elementary study of the function $t \mapsto \frac{3}{4} - \cos t + \frac{\cos 2t}{4}$ shows that it is always non negative. Since $v'' \leq 0$ because v has to be chosen concave, we see that D is necessarily non positive, what proves the desired result. $\square$

Finally, we calculated some points on the boundary of region $\mathcal{E}_C^N$ and we show the results in Figure 16. The boundary of the region $\mathcal{E}^N$, already plotted in Figure 12 is marked with a red dashed line.

References

[AA1] C. J. S. Alves and P. R. S. Antunes, The Method of Fundamental Solutions applied to the calculation of eigenfrequencies and eigenmodes of 2D simply connected shapes, Computers, Materials & Continua Vol 2, No. 4 (2005), 251–266.

[AA2] C. J. S. Alves and P. R. S. Antunes, The Method of Fundamental Solutions applied to some inverse eigenproblems, in preparation.

[AF1] P. Antunes and P. Freitas, New bounds for the principal Dirichlet eigenvalue of planar regions, Experiment. Math. **15** (2006), 333–342.

[AF2] P. Antunes and P. Freitas, A numerical study of the spectral gap, J. Phys. A **41** no.5, (2008), 055201, 19 pp.

[AV] P. R. S. Antunes and S. S. Valtchev, A Meshfree numerical method for acoustic wave propagation problems in planar domains with corners and cracks, J. Comp. Appl. Math. **234** (2010), 2646–2662.

[AB1] M. Ashbaugh and R. Benguria, Proof of the Payne-Pólya-Weinberger conjecture, Bull. AMS **25** (1991), 19–29.

[AB2] M. Ashbaugh and R. Benguria, A sharp bound for the ratio of the first two eigenvalues of the Dirichelt Laplacian and extensions, Ann. Math. **135** (1992), 601–628.

[AB3] M. Ashbaugh and R. Benguria, Universal bounds for the low eigenvalues of Neumann Laplacians in N dimensions, SIAM J. Math. Anal. **24** no 3 (1993), 557-570.

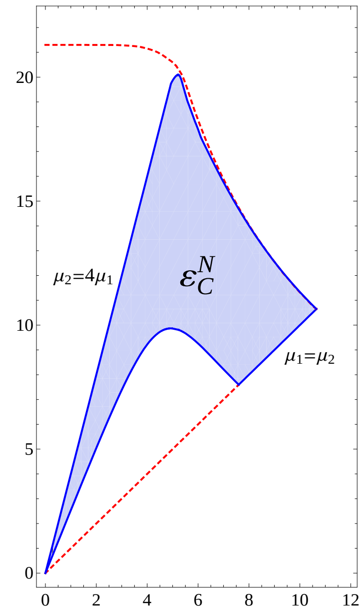

FIGURE 16. The region $\mathcal{E}_C^N$.

[B] T. Briançon, *Regularity of optimal shapes for the Dirichlet's energy with volume constraint*, ESAIM: COCV, **10** (2004), 99-122.

[BBF] D. Bucur, G. Buttazzo and I. Figueiredo, On the attainable eigenvalues of the Laplace operator, SIAM J. Math. Anal. **30** (1999), 527–536.

[C] D. Chenais, *On the existence of a solution in a domain identification problem*, J. Math. Anal. Appl., **52** (1975), 189-289.

[F1] G. Faber, Beweis, dass unter allen homogenen membranen von gleicher fläche und gleicher spannung die kreisförmige den tiefsten grundton gibt, Sitz. ber. bayer. Akad. Wiss. (1923), 169–172.

[GNP] A. Girouard, N. Nadirashvili and I. Polterovich, Maximization of the second positive Neumann eigenvalue for planar domains, arXiv:0803.4171,1-24.

[G] P.M. Gruber, The space of convex bodies, Handbook of convex geometry, P.M. Gruber and J.M. Wills eds, Elsevier 1993, pp. 301-318.

[H] A. Henrot, Extremum problems for eigenvalues of elliptic operators, Frontiers in Mathematics. Birkhäuser Verlag, Basel, 2006.

[HO1] A. Henrot and E. Oudet, Minimizing the second eigenvalue of the Laplace operator with Dirichlet boundary conditions, Arch. Rational Mech. Anal. **169** (2003), 73–87.

[HO2] A. Henrot and E. Oudet, Le stade ne minimise pas λ_2 parmi les ouverts convexes du plan, C. R. Acad. Sci. Paris Sér. I Math **332** (2001), 275–280.

[HP] A. Henrot and M. Pierre, Variation et optimisation de formes, Mathématiques et Applications **48**, Springer-Verlag, Berlin, 2005.

[J] D. Jerison, The direct method in the calculus of variations for convex bodies. Adv. Math. 122 (1996), no. 2, 262–279.

[KS] E. T. Kornhauser and I. Stakgold, A variational theorem for $\nabla^2 u + \lambda u = 0$ and its applications, J. Math. Physics **31** (1952), 45–54.

[K] E. Krahn, Über eine von Rayleigh formulierte minimaleigenschaft des kreises, Math. Annalen **94** (1924), 97–100.

[LS1] R.S. Laugesen and B.A. Siudeja, Minimizing Neumann fundamental tones of triangles: an optimal Poincaré inequality, Preprint. www.math.uiuc.edu/ laugesen/.

[LS2] R.S. Laugesen and B.A. Siudeja, Maximizing Neumann fundamental tones of triangles, Preprint. www.math.uiuc.edu/ laugesen/.

[LY] M. Levitin and R. Yagudin, Range of the first three eigenvalues of the planar Dirichlet Laplacian, LMS J. Comput. Math. **6** (2003), 1–17.

[M] E. Makai, On the principal frequency of a membrane and the torsional rigidity of a beam, in *Studies in mathematical analysis and related topics*, Essays in honor of George Pólya, Stanford Univ. Press, Stanford (1962), 227–231.

[O1] E. Oudet, Numerical minimization of eigenmodes of a membrane with respect to the domain, ESAIM Control Optim. Calc. Var. **10** (2004), 315–330.

[P1] G. Pólya, On the characteristic frequencies of a symmetric membrane, Math. Zeit. **63** (1955), 331–337.

[R] B. Rousselet, *Shape Design Sensitivity of a Membrane*, J. Opt. Theory and Appl., **40** (1983), 595-623.

[SZ] J. Sokolowski and J. P. Zolesio, Introduction to shape optimization: shape sensitity analysis, Springer Series in Computational Mathematics Vol 10, Springer, Berlin (1992).

[S] G. Szegö, Inequalities for certain eigenvalues of a membrane of given area, J. Rational Mech. Anal. **3** (1954), 343–356.

[T] B. A. Troesch, Elliptical membranes with smallest second eigenvalue, Math. Comp. **27** (1973), 767–772.

[W] H. F. Weinberger, An isoperimetric inequality for the N-dimensional free membrane problem, J. Rational Mech. Anal. **5** (1956), 633–636.

[WK] S. A. Wolf and J. B. Keller, Range of the first two eigenvalues of the Laplacian, Proc. Roy. Soc. London Ser. A **447** (1994), 397–412.

Group of Mathematical Physics of the University of Lisbon, Complexo Interdisciplinar, Av. Prof. Gama Pinto 2, P-1649-003 Lisboa, Portugal

E-mail address: `pant@cii.fc.ul.pt`

Institut Élie Cartan Nancy, UMR 7502, Nancy Université - CNRS - INRIA, B.P. 70239 54506 Vandoeuvre les Nancy Cedex, France

E-mail address: `henrot@iecn.u-nancy.fr`